THE JOURNAL OF BIOLOGICAL CHEMISTRY
Vol. 278, No. 29, Issue of July 18, pp. 26862–26869, 2003
Printed in U.S.A.

The ATP Hydrolysis Cycle of the Nucleotide-binding Domain of the Mitochondrial ATP-binding Cassette Transporter Mdl1p*

Received for publication, February 4, 2003, and in revised form, May 3, 2003
Published, JBC Papers in Press, May 13, 2003, DOI 10.1074/jbc.M301227200

Eva Janas, Matthias Hofacker, Min Chen, Simone Gompf, Chris van der Does‡, and Robert Tampé§

From the Institute of Biochemistry, Biocenter, J. W. Goethe-University, Marie-Curie-Str. 9, D-60439 Frankfurt a.M., Germany

The ABC transporter Mdl1p, a structural and functional homologue of the transporter associated with antigen processing (TAP) plays an important role in intracellular peptide transport from the mitochondrial matrix of *Saccharomyces cerevisiae*. To characterize the ATP hydrolysis cycle of Mdl1p, the nucleotide-binding domain (NBD) was overexpressed in *Escherichia coli* and purified to homogeneity. The isolated NBD was active in ATP binding and hydrolysis with a turnover of 25 ATP per minute and a K_m of 0.6 mM and did not show cooperativity in ATPase activity. However, the ATPase activity was non-linearly dependent on protein concentration (Hill coefficient of 1.7), indicating that the functional state is a dimer. Dimeric catalytic transition states could be trapped either by incubation with orthovanadate or beryllium fluoride, or by mutagenesis of the NBD. The nucleotide composition of trapped intermediate states was determined using [α-^{32}P]ATP and [γ-^{32}P]ATP. Three different dimeric intermediate states were isolated, containing either two ATPs, one ATP and one ADP, or two ADPs. Based on these experiments, it was shown that: (i) ATP binding to two NBDs induces dimerization, (ii) in all isolated dimeric states, two nucleotides are present, (iii) phosphate can dissociate from the dimer, (iv) both nucleotides are hydrolyzed, and (v) hydrolysis occurs in a sequential mode. Based on these data, we propose a processive-clamp model for the catalytic cycle in which association and dissociation of the NBDs depends on the status of bound nucleotides.

ATP-binding cassette (ABC)[1] transporters comprise a large family of membrane proteins that catalyze the active transfer of a variety of solutes across biological membranes (1). The function of ABC transporters is central to various human pathologies such as cystic fibrosis, adrenoleukodystrophy, retinal dystrophies, and multidrug resistance. The transporter associated with antigen processing (TAP) is an ABC transporter in vertebrates, which translocates peptides from the cytosol into the ER and performs a key function in the antigen presentation and adaptive immune response (2). Recently, a close homologue, Mdl1p (multidrug resistance like), localized in the inner mitochondrial membrane of *Saccharomyces cerevisiae*, has been identified as an intracellular peptide transporter (3). This transporter exports peptides derived from the degradation of non-assembled membrane proteins. These peptides are generated by ATP-dependent m-AAA (matrix-oriented ATPases associated with a variety of cellular activities) proteases, which mediate the degradation and turnover of inner mitochondrial membrane proteins and short-lived regulatory proteins in an ubiquitin/proteasome-independent manner (4). Protein fragments with a length of 6–21 amino acids are released by Mdl1p into the intermembrane space (3).

Half-size ABC transporters, like the heterodimeric TAP and homodimeric Mdl1p, have a common molecular architecture consisting of two polytopic transmembrane domains (TMD) and two nucleotide-binding domains (NBD). The transmembrane domains interact with the substrates and form the substrate translocation pore across the membrane. The TMDs generally share little homology (5), probably caused by the broad substrate spectrum of the ABC transporter family. Binding and hydrolysis of nucleotides drive the transport process by transducing conformational changes from the NBDs to the TMDs. The similarity of different NBDs is significantly higher compared with the TMDs, suggesting that even in transporters of unrelated function the structure and function of the NBDs be highly conserved. Each NBD contains a highly conserved Walker A and Walker B motif (6) characteristic of ATP-binding P-loop proteins, as well as the C-loop motif (LSGGQ) unique to ABC proteins, which is also known as the ABC signature motif. The crystal structures of bacterial ABC transporters (*e.g.* MsbA, BtuCD) and of isolated NBDs (*e.g.* HisP, MalK, MJ1276, and TAP1) show a consensus fold for the monomer (7–14). This fold shows an L-shaped molecule with two arms, one including the ATP-binding domain containing the Walker A and B motifs, and the other including the ABC signature motif (7). The crystal structures of several NBD dimers have been solved, but they differ significantly in the manner the monomers are associated (15, 16). The crystal structure of the ATP-bound Rad50 dimer, a DNA repair enzyme that shares homology with the NBDs of ABC proteins is assumed to be the physiologically relevant dimer. This dimer contains two nucleotides, which are clamped at the interface between two monomers causing them to dimerize in a head-to-tail manner (17). The ATP molecules are sandwiched between the Walker A and B motifs from one monomer and the C-loop from the other monomer. This pro-

* The work was supported by the Deutsche Forschungsgemeinschaft. The costs of publication of this article were defrayed in part by the payment of page charges. This article must therefore be hereby marked "*advertisement*" in accordance with 18 U.S.C. Section 1734 solely to indicate this fact.

‡ Supported by a TALENT fellowship from the Netherlands Organization for Scientific Research (NWO).

§ To whom correspondence should be addressed. Tel.: 49-69-798-29475; Fax: 49-69-798-29495; E-mail: tampe@em.uni-frankfurt.de.

[1] The abbreviations used are: ABC, ATP-binding cassette; AMP-PNP, 5′-adenylyl-β,γ-imidodiphosphate; ATPγS, adenosine 5′-*O*-(3-thio)triphosphate; ER, endoplasmic reticulum; IC_{50}, 50% inhibitory concentration; mAAA, matrix-oriented ATPases associated with a variety of cellular activities; MALDI-TOF MS, matrix-assisted laser desorption/ionization-time of flight mass spectrometry; NBD, nucleotide-binding domain; PBS, phosphate-buffered saline; P-gp, P-glycoprotein; TMD, transmembrane domain; TLC, thin layer chromatography; TAP, transporter associated with antigen processing.

posed functional dimer configuration was also found in the crystal structure of a mutant NBD from *Methanococcus jannaschii* MJ0796 (14) and in the NBD of the full-length bacterial vitamin B_{12} transporter BtuCD (13). Biochemical data on NBDs like MalK or of P-gp further confirmed the involvement of the C-loop in ATP binding (18, 19). The dimer is generally regarded as the ATPase active form of ABC transporters, but it remains controversial at which point of the transport cycle the dimer is formed and how both NBDs cooperate. Whether the motor domains work as equivalent modules, hydrolyzing both ATP synchronously, sequentially or alternatively is still under discussion. It is also not clarified how ATP hydrolysis powers the substrate translocation. Based on the P-gp ATPase cycle, it was suggested that hydrolysis of one ATP provides energy for the translocation of the substrate whereas hydrolysis of the ATP in the second binding pocket might have regulatory functions, possibly returning the complex to the starting point of the ATPase cycle (20, 21).

To obtain insight into the mechanism of the NBDs, we expressed and purified the NBD of Mdl1p. Either by incubation with orthovanadate or beryllium fluoride, or by mutagenesis of the NBD, catalytic transition states were trapped and the nucleotide composition of these states was analyzed. Based on these results, we propose a new model for the ATPase cycle combining structure and function of the ABC dimer.

EXPERIMENTAL PROCEDURES

Heterologous Expression of Mdl1p-NBD in Escherichia coli—The C-terminal domain (amino acids 423–695) of Mdl1p (ORF YLR188W) was amplified by PCR on genomic DNA of *S. cerevisiae* using the following primers: 5′-TCCGACTATTGGAAAGGATCCTGTGTC-3′; 5′-TACTCGAGAAGCTTTATACTTCC CGGGCAACACTAT-3′ and cloned into the *Bam*HI and *Hind*III sites of pET28b (Novagen). The resulting plasmid (pET-NBD) includes the NBD with an N-terminal His_6 tag, a thrombin cleavage site and a T7 tag encoded by the vector. A conserved glutamate (E599Q, GAA->CAA) one amino acid downstream of the Walker B motif was changed to glutamine via PCR mutagenesis resulting in pET-NBD(E599Q). *E. coli* strain BL21(DE3) (Novagen) was transformed with the plasmids and grown in LB medium with 50 μg/ml kanamycin at 30 °C. At an OD_{600} of 0.5 the cells were induced with 0.2 mM isopropyl-β-D-thiogalactopyranoside, and after 3 h the cells were harvested by centrifugation.

Purification of Mdl1p-NBD—The cell pellet was resuspended in lysis buffer (PBS: 10 mM Na_2HPO_4/NaH_2PO_4, pH 7.6, 150 mM NaCl, 5 mM KCl), 20 mM imidazole containing 1 mM phenylmethylsulfonylfluoride, 1% lysozyme, and 5–10 units of benzonase (Merck) and disrupted by French press treatment at 1,000 p.s.i. After centrifugation for 30 min at 100,000 × *g*, the supernatant was applied on a Ni-IDA column (Amersham Biosciences) preequilibrated in PBS supplemented with 20 mM imidazole. The column was washed with step gradients of 80 and 100 mM imidazole in PBS, and the protein was eluted with 250 mM imidazole. Fractions containing the NBD were pooled, concentrated by Centricon 10 (Millipore), and applied to a Superdex 200 HR 26/60 prep grade gel filtration column (Amersham Biosciences) in 20 mM Tris, pH 8.0, 100 mM NaCl. The NBD eluted with an apparent molecular weight of 33 kDa corresponding to the size of the monomer. Fractions were concentrated to 10 mg/ml and stored at 4 °C. Wild-type and mutant proteins were purified to greater than 99% homogeneity as assessed by Coomassie-stained protein on SDS-PAGE (15%) and MALDI-TOF MS.

8-Azido-ATP Photolabeling—After preincubation of the purified NBD (0.3 μM) with different concentrations of nucleoside tri/diphosphates for 5 min in binding buffer (20 mM Tris, pH 8.0, 100 mM NaCl, 5 mM $MgCl_2$, 1 mM $MnCl_2$) on ice, 8-azido-[α-^{32}P]ATP was added to a final concentration of 0.5 μM and incubation was continued on ice for 5 min. Samples were irradiated by UV (254 nm) for 5 min, directly resuspended in SDS loading buffer, and separated by 15% SDS-PAGE. The gel was dried and quantified by phosphor imaging. The data were fitted to the Hill equation $y = (ax^n/(b^n + x^n))$, resulting both for ATP and ADP in a best fit ($R^2 = 0.98$) with a Hill coefficient (n) of 1.

ATPase Assay—ATPase activities were measured by the malachite green assay as described previously (22). The ATPase assay was performed in 20 mM Tris, pH 9.0, 100 mM NaCl and 15 mM $MgCl_2$ with 0–150 μM NBD for either 2 min at 16 °C (high NBD concentrations) or 4 min at 30 °C. The reaction was started by the addition of ATP to final concentrations of 0 to 10 mM. Data were fitted to the Hill equation $y = (ax^n/(b^n + x^n))$. The ATPase activity of the E599Q mutant was determined using radiolabeled ATP. Shortly, E599Q NBD (250 μM) was incubated in 20 mM Tris, pH 9.0, 100 mM NaCl, and 15 mM $MgCl_2$ at 30 °C. The reaction was started by addition of 2 mM MgATP supplemented with 0.04 μM [γ-^{32}P]ATP (4500 Ci/mmol, ICN). Samples were taken at different time points (0–200 min), separated by thin layer chromatography (see below) and the rate of released radioactive phosphate was quantified by a phosphorimager. As a negative control, spontaneous ATP hydrolysis was tested in the presence of heat-inactivated NBD.

Dimerization Assays—Before use, orthovanadate stock solution adjusted to pH 8.0 was boiled for 5 min to break polymeric species (23). Before use, beryllium fluoride solution was prepared by mixing $BeCl_2$ and NaF in a ratio of 1:100. For non-radioactive assays, purified wild-type NBD (30 μM) was incubated with different concentrations of beryllium fluoride (BeF_x) or orthovanadate in the presence or absence of nucleotides and nucleotide analogues for 5 min at 30 °C in binding buffer. The mutant NBD (E599Q, 30 μM) was incubated for 5 min under non-hydrolyzing conditions (in the absence of Mg^{2+} and on ice) or ATP hydrolysis conditions (in the presence of 5 mM Mg^{2+} and at 30 °C) with different concentrations of nucleotides and nucleotide analogues. The samples were applied to a Superdex 75 PC 3.2 (Amersham Biosciences) gel filtration column at a flow rate of 50 μl/min at 4 °C in 20 mM, Tris pH 8.0, 150 mM NaCl, and 5 mM $MgCl_2$ if indicated.

Determination of the Nucleotide Stoichiometry—Radioactive trapping experiments, were performed in the same buffer as non-radioactive trapping experiments, and separated by gel filtration. Fractions were analyzed by β-counting, thin layer chromatography, and for protein concentration by the BCA assay (Pierce). Over the range of protein concentrations used, the A_{280} measured with the UV detector of the SMART system (Amersham Biosciences) was linearly related to the protein concentration determined by the BCA assay. In particular, wild-type NBD (250 μM) was incubated with 500 μM MgATP supplemented with 0.1 μM of either [α-^{32}P]ATP or [γ-^{32}P]ATP (4500 Ci/mmol, ICN) in the presence of BeF_x (500 μM) for 5 min at 30 °C. The E599Q mutant (250 μM) was incubated for 5 min in the absence of Mg^{2+} and on ice. To follow one to two turnovers of the E599Q mutant, 250 μM NBD were incubated for prolonged time periods (0–500 min) at 30 °C with limiting concentration of MgATP (250–500 μM) and tracer amounts of radioactive ATP. To test whether ADP is incorporated in the dimer at a high ADP concentration, the E599Q mutant was incubated with 500 μM ADP and 0.1 μM [α-^{32}P]ADP in the presence of various concentration of unlabeled ATP (0, 5, 50, 100, and 500 μM) for 10 min at 30 °C. Alternatively, incorporation of ADP under limiting concentrations of MgATP was tested by incubating the E599Q mutant (250 μM) with MgATP (250–500 μM) supplemented with tracer amounts of [α-^{32}P]ADP at 30 °C for 400 min. The [α-^{32}P]ADP was formed by incubation of [α-^{32}P]ATP with hexokinase (Sigma Aldrich) according to the manufacturer's instructions, separated from hexokinase by Centricon 10 centrifugation, and full conversion to [α-^{32}P]ADP was confirmed by TLC.

Thin Layer Chromatography—The nucleotide composition of the dimer was analyzed by TLC. Immediately after gel filtration the fraction containing the dimer was incubated with 15 mM EDTA for 30 min and precipitated with trichloroacetic acid (10% w/v) for 30 min at 4 °C. After centrifugation at 20,000 × *g* for 5 min, the sample was neutralized with 0.5 M $KHCO_3$, pH 8.3 and applied onto polyethylenimine cellulose plates (Merck) in 2 M formate and 250 mM LiCl. [α-^{32}P]ATP and [γ-^{32}P]ATP treated with hexokinase were used as references.

RESULTS

Purification and Activity of NBD of Mdl1p—ABC transporters undergo a series of conformational changes in response to ATP binding and hydrolysis at the NBDs, and binding, transport and release of substrate at the TMDs. Various aspects of the mechanism how the motor domains of ABC transporters work can be learned from the isolated NBDs. Therefore, the NBD of the mitochondrial half-size ABC transporter Mdl1p was cloned, expressed in *E. coli* and purified to homogeneity (Fig. 1, *left panel*). About 50 mg of soluble and purified protein at 10 mg/ml was obtained from a 1-liter culture. The identity of the sample was confirmed by MALDI-TOF MS (data not shown). The activity of the isolated wild-type NBD was analyzed with respect to ATP and ADP binding using 8-azido-[α-^{32}P]ATP photolabeling experiments. Photolabeling with

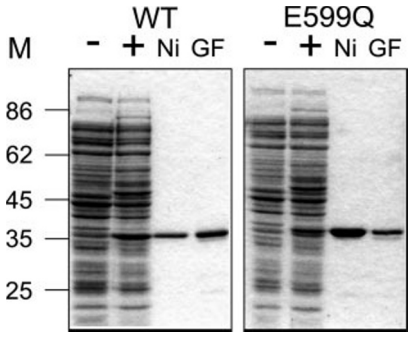

FIG. 1. **Heterologous expression and affinity purification of wild-type (*WT*) and mutant (E599Q) NBD of Mdl1p.** Coomassie-stained 15% SDS-PAGE containing crude extract of non-induced (−) and induced (+) cells, purified NBD after Ni^+-chelating affinity purification (*Ni*) and gel filtration (*GF*). *M* indicates protein marker in kDa.

8-azido-[α-^{32}P]ATP was specifically competed by excess of unlabeled nucleoside di/triphosphates (Fig. 2*A*). The IC_{50}, roughly reflecting the K_d value, was determined to be 2 μM for MgATP and 64 μM for MgADP (Fig. 2*B*). The absence of Mg^{2+} dramatically reduced the affinity of nucleotides to the NBD. The affinity for MgCTP, MgGTP, MgUTP was ~30-fold lower compared with MgATP (data not shown). The isolated NBD was active in ATP hydrolysis (30 μM NBD, Fig. 3*A*) with a K_m, ATP of 0.6 mM and showed no cooperativity with increasing ATP concentration (Hill coefficient of 1.0, Fig. 3*A*, *inset*). However, the ATPase activity was observed to be non-linearly dependent on protein concentration. The specific ATPase activity increased over two orders of magnitude at higher protein concentrations. At concentrations higher than 250 μM the NBD precipitated. Based on a V_{max} of 25 ATP/NBD/min, a $K_{0.5\ NBD}$ of 75 μM and a Hill coefficient of 1.7 (Fig. 3*B*, *inset*) were determined, suggesting that the active form of the enzyme is a dimer. Also at low (5 μM) and high (150 μM) NBD concentrations, the K_m, ATP was 0.6 mM and showed no cooperativity with increasing ATP concentration (data not shown). The NBD had a maximal ATPase activity at a pH of 8–9 (data not shown), comparable to the pH of the mitochondrial matrix.

The Active Form of NBD Is a Dimer—It is postulated that the interaction of both NBDs plays a central role in the catalytic cycle of ABC transporters (see review in Ref. 24). So far, gel filtration experiments with isolated NBDs (*e.g.* HisP or NBDs of P-gp) could not demonstrate ATP-dependent dimerization, independent of the presence of nucleotides or non-hydrolyzable analogues such as AMP-PNP (25, 26). The wild-type NBD of Mdl1p also behaved as a monomer in gel filtration studies independent of the presence of nucleotides. To analyze intermediate states of the ATPase cycle, we tried to trap the NBD in the conformation directly after ATP hydrolysis using orthovanadate (V_i) or beryllium fluoride (BeF_x). As shown on myosin x-ray structures the vanadate-inhibited complex resembles a post-hydrolysis state while the complex trapped by BeF_x represents a pre-hydrolysis state (27). After 5 min of preincubation of the NBD with BeF_x in the presence of MgATP at 30 °C, a stable dimer corresponding to a molecular mass of 66 kDa was observed by gel filtration even in the absence of MgATP and BeF_x in the mobile phase (Fig. 4*A*). The formation of the dimer was dependent on the concentration of BeF_x. At a concentration of 1 mM BeF_x almost 80% of the protein was detected as a dimer. The same result was observed with orthovanadate (Fig. 4*B*). Importantly, neither preincubation of the NBD with MgADP or MgAMP-PNP in the presence of BeF_x/vanadate at 30 °C, nor incubation with MgATP and BeF_x/vanadate at 4 °C induced dimerization of NBD. Omitting Mg^{2+} from the reaction inhibited the formation of dimers. This demonstrates that ATP hydrolysis is essential for the formation of the BeF_x/vanadate-stabilized dimer.

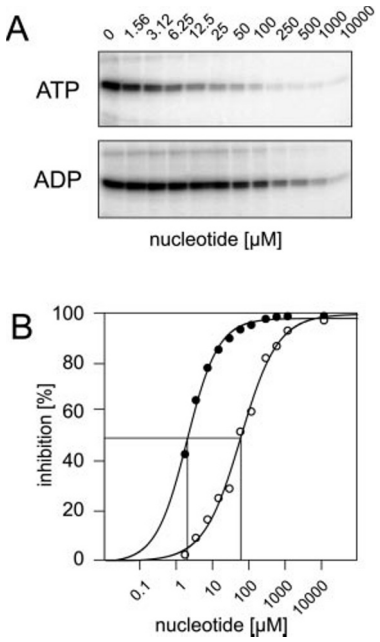

FIG. 2. **8-Azido-[α-^{32}P]ATP photolabeling of purified wild-type NBD of Mdl1p.** *A*, competition of 8-azido-[α-^{32}P]ATP (0.5 μM) photolabeling of wild-type NBD with increasing amounts of MgATP (*closed circles*) or MgADP (*open circles*). *B*, quantification of photolabeling efficiency by phosphorimager. The data were fitted to the Hill equation $y = (ax^n/(b^n + x^n))$ resulting both for ATP and ADP in a best fit (R^2 = 0.98) with a Hill coefficient (n) of 1.

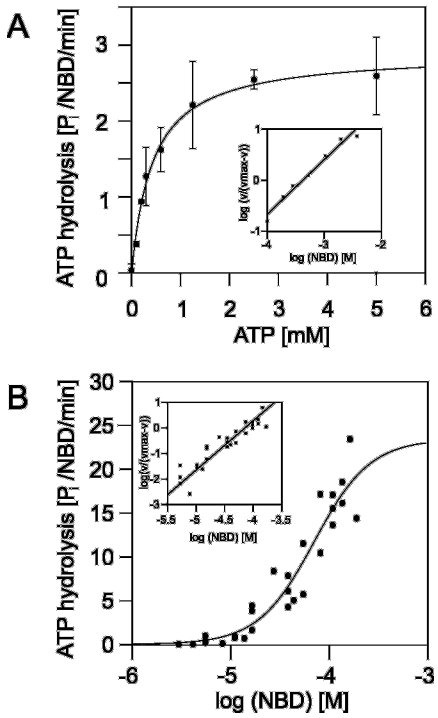

FIG. 3. **ATPase activity of wild-type NBD of Mdl1p.** *A*, ATPase activity as a function of the ATP concentration measured at 30 °C with 30 μM NBD. The *inset* shows the same data plotted according to the Hill equation (Hill coefficient = 1.0). *B*, ATPase activity as a function of the NBD concentration (0–150 μM) measured in the presence of 10 mM ATP. The *inset* shows the same data plotted according to the Hill equation (Hill coefficient = 1.7).

ATP-dependent Dimerization of the E599Q Mutant NBD—Exchange of the conserved glutamate downstream of the

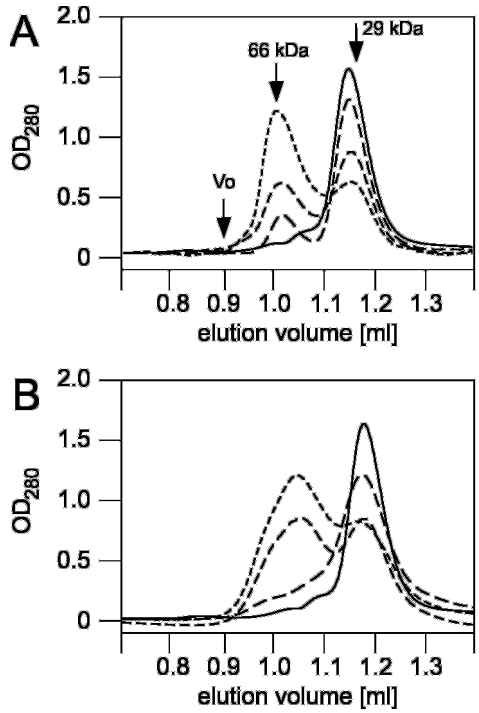

FIG. 4. **BeF_x-dependent formation of the ATP-induced dimer.** *A,* after preincubation of the wild-type NBD (30 μM) with increasing concentrations of BeF_x (0 mM, *straight line*; 0.25 mM, *long dash*; 0.5 mM, *intermediate dash*; and 1 mM, *short dash*) for 5 min at 30 °C in the presence of MgATP (500 μM), the formation of the dimer was monitored by gel filtration. *B,* after preincubation of the wild-type NBD (30 μM) with increasing concentrations of orthovanadate (0 mM, *straight line*; 0.5 mM, *long dash*; 2.5 mM, *intermediate dash*; and 5 mM, *short dash*) for 5 min at 30 °C in the presence of MgATP (500 μM), the formation of the dimer was monitored by gel filtration. *Arrows* indicate void volume (V_o), and column calibration standards bovine serum albumin (66.0 kDa) and carbonic anhydrase (29.0 kDa).

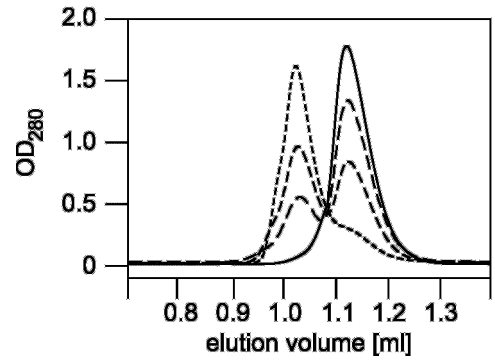

FIG. 5. **ATP-dependent dimerization of the E599Q mutant.** After preincubation of E599Q mutant (30 μM) with increasing concentrations of MgATP (0 μM, *straight line*; 20 μM; *long dash*; 200 μM, *intermediate dash*; and 500 μM *short dash*) for 5 min on ice, the formation of the dimer was monitored by gel filtration.

Walker B motif (E552Q/E1197Q) of mouse P-gp produced an ABC transporter with severely impaired biological activity and no substrate-stimulated ATPase activity (28). Equivalent mutation of the archaeal NBDs of MJ0796 and MJ1267 (E171Q/E179Q) induced an ATP-dependent dimerization of the NBDs (29). We introduced an equivalent mutation in the conserved glutamate (E599Q) in the NBD of Mdl1p, which was expressed and purified in equal amounts as the wild-type protein (Fig. 1). The mutant NBD bound ATP to the same extent as the wild-type as analyzed by 8-azido-ATP photolabeling experiments (data not shown). As expected, no steady-state ATP hydrolysis was observed by measuring the release of P_i using the malachite green assay (data not shown). To assay the ability of the mutant to form nucleotide-dependent dimers, we incubated the mutant NBD with MgATP on ice for 5 min. Gel filtration experiments showed that MgATP induced dimerization in a concentration-dependent manner (Fig. 5). The E599Q NBD dimer was stable during gel filtration even without nucleotides in the mobile phase, indicating that the ATP-induced dimer only slowly dissociates. Importantly, ADP did not induce dimerization, and the addition of ADP to the monomers impaired ATP-dependent dimer formation. Addition of Mg^{2+} (0–5 mM) did not influence the dimerization. Furthermore, MgAMP-PNP or MgATPγS could bind to the wild-type and mutant NBD of Mdl1p to the same extent as MgATP, but did neither induce dimerization of the wild-type NBD nor of the E599Q mutant (data not shown). Based on these results we can conclude that presence of ATP is absolutely required for the formation of both wild-type and mutant dimer.

Nucleotide Composition of the Dimer—To analyze the ATP/ADP composition of the nucleotide-induced dimer, wild-type NBD was incubated with tracer amount of either [α-^{32}P]ATP or [γ-^{32}P]ATP under BeF_x-trapping conditions and applied to the gel filtration column. Radioactive nucleotides exclusively co-eluted with the dimer, whereas no radioactive nucleotides were observed in fractions corresponding to the monomer (Fig. 6*A*). The amount of [α-^{32}P]ATP bound per wild-type dimer was determined and a stoichiometry of two nucleotides per dimer was obtained (Fig. 6*A*, *open circles*). Trapping the NBD by BeF_x in the presence of [γ-^{32}P]ATP resulted in a dimer with almost no radioactive nucleotides incorporated (Fig. 6*A*, *filled circles*, Table I). These results demonstrate that two ATP molecules are already hydrolyzed in the BcF_x-trapped wild-type dimer and the [γ-^{32}P]$_i$ is released from the complex. This was confirmed by TLC analysis (Fig. 6*A*). Under the same conditions, incorporation of [α-^{32}P]ADP into the dimer was not observed, even in the presence of different concentrations of ATP (data not shown).

In experiments with the E599Q mutant, performed at 4 °C and in the absence of Mg^{2+}, the nucleotides exclusively co-eluted with the dimer as well. In this experiment, the amount of both [α-^{32}P]ATP and [γ-^{32}P]ATP bound per dimer was equal and a stoichiometry of two ATP molecules per dimer was obtained (Fig. 6*B*, Table I). TLC clearly demonstrated that ATP and not ADP and P_i were incorporated into the dimer. As mentioned above, incubation with non-hydrolyzable ATP analogues did not trigger dimer formation.

Our data from both the BeF_x-trapped wild-type NBD and the E599Q mutant suggest that during the ATP hydrolysis cycle at least two different intermediate states can be isolated. Importantly, both states contain two nucleotides. In one state the nucleotides are bound as ATP as shown for the E599Q mutant. In the other state both nucleotides have been hydrolyzed to ADP and P_i as demonstrated for the trapped wild-type NBD. This suggests that ATP binding on both NBDs induces formation of the dimer and that after hydrolysis of both ATP molecules to ADP, the dimeric complex dissociates and ADP is released.

Hydrolysis Cycle of the E599Q Mutant—An important remaining question is how the ATPs are hydrolyzed during one cycle. Using radiolabeled ATP, it was determined that the E599Q mutant, at 30 °C and in the presence of Mg^{2+} was still able to hydrolyze ATP with a turnover rate of 0.5 ATP per hour (data not shown). The ATPase activity of the E599Q mutant was 3000-fold reduced compared with the wild-type. The amount of released phosphate in the radioactive ATPase assay increased linearly over several hours, indicating that the E599Q mutant can make multiple turnovers. The strongly

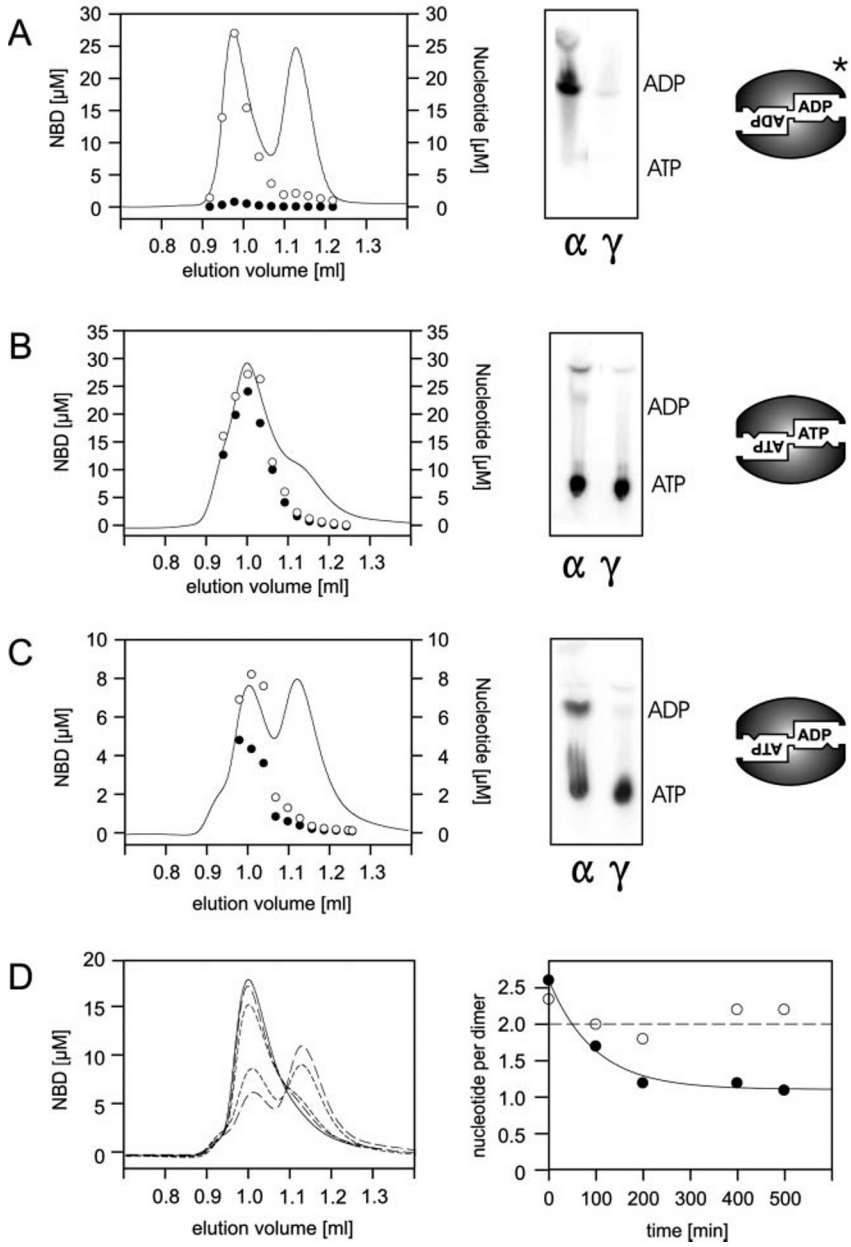

FIG. 6. **Nucleotide stoichiometry of trapped NBDs.** *A*, wild-type NBD (250 μM) was trapped using MgATP (500 μM) and BeF_x (500 μM) for 5 min at 30 °C in the presence of tracer amounts of either [α-^{32}P]MgATP (*open circles*) or [γ-^{32}P]-MgATP (*closed circles*), and separated by gel filtration (*left panel*). The nucleotide concentration was determined by β-counting and the protein concentration (*straight line*) by the BCA assay and by measuring A_{280}. On the *middle panel*, TLC of the nucleotides incorporated into the dimer is shown. *B*, E599Q mutant (250 μM) was trapped with ATP (500 μM) and tracer amounts of either [α-^{32}P]ATP (*open circles*) or [γ-^{32}P]ATP (*closed circles*) in the absence of Mg^{2+} for 5 min on ice, and separated by gel filtration (*left panel*). The nucleotide and protein concentration was determined as above. The *middle panel* shows the TLC of the nucleotides incorporated into the dimer. *C,* to isolate the E599Q dimer under ATP limiting conditions, the E599Q mutant (250 μM) was preincubated with ATP (250 μM) and tracer amounts of [α-^{32}P]ATP or [γ-^{32}P]ATP at 30 °C for 400 min in the presence of Mg^{2+}, and isolated by gel filtration. The nucleotide and protein concentration was determined as above. The *middle panel* shows the TLC of the nucleotides incorporated into the dimer. *D*, *left panel*; the dimer dissociation of the E599Q mutant was monitored by gel filtration after incubation under ATP-limiting conditions (see *C*) for the indicated time (0 min, *straight line*; 100 min, *long dash*; 200 min, *intermediate-long dash*; 400 min, *intermediate dash*; 500 min, *short dash*). *Right panel*, the ATP/ADP composition of the isolated dimers was analyzed as described above. *Schemes* on the right of 6*A*, 6*B*, and 6*C* depict the isolated states. *, the BeF_x-trapped state.

TABLE I
Nucleotide composition of the dimer (average of 5 experiments)

Nucleotide/dimer	Wild-type 30°C, BeF_x-trapped	E599Q 4°C, no Mg^{2+}, ATP	E599Q 30°C, Mg^{2+}, limiting ATP
mol/mol			
[γ-^{32}P]ATP	0.01 ± 0.01	2.50 ± 0.18	1.16 ± 0.06
[α-^{32}P]ATP	1.76 ± 0.06	2.27 ± 0.15	2.18 ± 0.14
[α-^{32}P]ADP			0.02 ± 0.02

reduced turnover rate gave us a tool to examine the hydrolysis cycle in more detail. When the dimer was incubated with limiting amounts of ATP at 30 °C in the presence of Mg^{2+} in order to allow only one or two ATP hydrolysis turnovers, the gel filtration analysis of the E599Q mutant showed that, over time, the amount of dimeric NBD decreases and the amount of monomeric NBD increases (*e.g.* after 400 min, Fig. 6, *C* and *D*, *left panel*). The nucleotide composition of the remaining dimer was analyzed, and was found to contain one ATP and one ADP (Fig. 6*C*, Table I). TLC analysis of the dimer confirmed an intermediate state containing equal amount of ATP and ADP (Fig. 6*C*, *middle panel*). The dimers isolated after prolonged incubation times at 30 °C (Fig. 6*D*, *left panel*) reached a stoichiometry of one ATP and one ADP (Fig. 6*D*, *right panel*), suggesting that this is a stable intermediate state, which can be detected under limiting ATP conditions. To exclude that the ADP found in the dimer is derived from ADP rebinding from the solution, ADP incorporation was followed under exactly the same conditions using [α-^{32}P]ADP as a tracer. Under these conditions no incorporation of [α-^{32}P]ADP was detected (Table I). This demonstrated that the dimer-bound ADP is derived from hydrolysis of the first ATP. The intermediate state suggests that the ATP hydrolysis occurs by a sequential mechanism, and that in the E599Q mutant hydrolysis of the second ATP is slower than hydrolysis of the first.

DISCUSSION

Several crystal structures showed that the catalytic pocket for ATP hydrolysis is produced only by the cooperation of two NBDs (13, 14, 17), explaining the positive cooperativity in ATPase activity observed for $MalFGK_2$ and $HisQMP_2$ (30–32). The residues involved in ATP binding and subsequent dimerization of the NBDs have been characterized (18, 19, 29). Al-

though it is widely agreed that the dimer is a functional intermediate, several models have been proposed for the mechanism by which ATP drives the translocation of the substrate (see below). Although it was previously reported that NBDs form dimers (33), it was not elucidated how dimerization of the NBDs is coordinated by nucleotides during one catalytic cycle. Here, for the first time, several different intermediate states in the hydrolysis cycle of NBD-Mdl1p were isolated and directly analyzed for their nucleotide content. Based on these data we propose a new model for the hydrolysis cycle of an ABC transporter, unifying structural and functional data.

Mdl1p has recently been identified as an intracellular homodimeric half-size ABC transporter localized in the inner mitochondrial membrane of *S. cerevisiae* (3). The peptide transporter Mdl1p shares functional and structural homology to the heterodimeric TAP. We are interested in the mechanism of peptide transport across membranes, and especially how ATP drives this transport. As the Mdl1p transporter is proposed to work as a homodimer, we chose the NBD of Mdl1p as a model. This is the first report with mechanistic data on Mdl1p, and no *in vitro* data are presently available for the full-length Mdl1p. The C-terminal domain (amino acids 427–695) corresponding to the NBD was overexpressed as soluble protein in *E. coli* and purified to homogeneity. The purified NBD was active in ATP binding and hydrolysis. The turnover number of the Mdl1p-NBD (25 min^{-1}) is comparable to the values obtained for other isolated NBDs (*e.g.* MJ0796, 12 min^{-1}, Ref. 29, CFTR, 6.7 min^{-1}, Ref. 34). In general, isolated NBDs show much lower turnover numbers than the full-length transporters, and no substrate stimulation (26). The ATPase activity of isolated Mdl1p-NBD was observed to be non-linearly dependent on protein concentration, indicating that the active form of Mdl1p is a dimer. Surprisingly, the NBD did not reveal positive cooperativity with increasing ATP concentration. This is in contrast to the behavior of isolated MJ0796 NBD, which showed positive cooperativity with a Hill coefficient of 1.7 (29). However, in agreement with our data, other isolated NBDs like HisP and MalK displayed no cooperativity for ATP, while cooperativity in ATPase activity was determined in the fully assembled transporters $HisQMP_2$ and $MalFGK_2$ (25, 30). This different behavior of various ABC transporters shows that although dimerization of the NBDs is proposed for all, there are differences in the cooperativity of the NBDs, which in some cases might be caused by the TMDs.

The NBD of Mdl1p behaved as a monomer in gel filtration studies independent of the presence of nucleotides as previously shown for other isolated NBDs (25). For the first time, an NBD of an ABC transporter was trapped as a dimer using either orthovanadate or beryllium fluoride. ADP could not replace ATP in the trapping reaction, demonstrating that ATP binding and hydrolysis are essential for dimerization. Even in the absence of orthovanadate or BeF_x, an ATP-dependent dimer was obtained by mutation of the conserved glutamate downstream of the Walker B motif of Mdl1p (E599Q). The formation of stable dimers upon ATP binding was very recently described by gel filtration of mutant archaeal NBDs (MJ0796-E171Q/MJ1267-E179Q) (29). These mutants were deficient in steady-state ATPase activity as assayed by standard ATPase assays (P_i or ADP release) as were the equivalent mutants (E552Q/E1197Q or E556Q/E1201Q) of human and mouse P-gp (21, 28). The structures of some ABC transporters have suggested that this conserved glutamate is the most likely candidate to play the role of the catalytic carboxylate (7–9, 11, 14, 17). During preparation of this manuscript, this glutamate of human P-gp was suggested not to function in the cleavage between γ and β phosphate, but to be part of the switch region

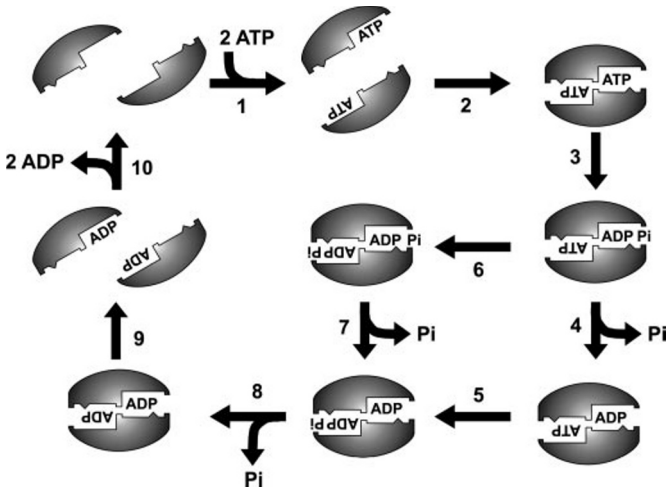

FIG. 7. **A processive clamp model for the ATPase cycle of the NBD from the ABC transporter Mdl1p.** ATP binding (*step 1*) on both NBD monomers induces formation of the dimer (*step 2*). After ATP hydrolysis by the first NBD (*step 3*), either the P_i is released first (*step 4*), followed by hydrolysis of the second ATP (*step 5*) and release of the second P_i (*step 8*), or the second ATP is hydrolyzed first (*step 6*) and then both phosphates are set free (*steps 7* and *8*). After both ATPs are hydrolyzed to ADP and both phosphates are released, the dimeric complex dissociates (*step 9*) and ADP (*step 10*) is released. The hydrolysis cycle can then start again with ATP binding. Not depicted in the figure: BeF_x or orthovanadate trapped the wild-type NBD in the intermediate state with two bound ADPs. Mutation of the catalytic glutamate resulted in E599Q NBD, which under non-hydrolysis conditions was trapped with 2 ATPs inside the dimer and under hydrolysis conditions one ADP along with one ATP molecule was incorporated into the dimer.

of ABC transporters possibly involved in the transmission of interdomain signals from the substrate-binding site to NBDs (21).

In this study, the nucleotide composition of the trapped states of Mdl1p was analyzed in detail by incorporating [α-^{32}P]ATP or [γ-^{32}P]ATP into the dimer. After gel filtration, the nucleotide concentration was analyzed by β-counting and correlated to the protein concentration. The nucleotide species were identified by TLC. Radioactive nucleotides were exclusively associated with the dimers. This observation demonstrated that ATP binding to the monomer is transient resulting in either subsequent dimerization of the NBDs or dissociation of ATP from the monomer. It was previously shown that non-trapped NBDs have very fast k_{off} rates for nucleotide binding (23). Radioactive ADP in the presence of various concentrations of ATP was not incorporated into the dimer. Based on these results, ATP binding is regarded as essential and sufficient for dimerization of the mutant. Interestingly, although AMP-PNP or ATPγS binds with similar affinity to the E599Q mutant as ATP, none of these analogues was able to induce ATP-dependent dimerization. This observation is in line with results obtained on mutants from *M. jannaschii* (29). Incubation of the wild-type NBD of Mdl1p with an equimolar ratio of unlabeled MgATP and MgATPγS under BeF_x-trapping conditions did not result in any incorporation of ATPγS in the dimer. This suggests that either the dimer interface is disturbed in the presence of ATPγS, or both nucleotides have to be hydrolyzed to obtain the BeF_x-trapped intermediate. Analysis of the dimer always showed two nucleotides bound per dimer. In case of the BeF_x-trapped NBD the nucleotide species was exclusively ADP (with no P_i in the dimer), while in the E599Q mutant exclusively two ATP molecules were incorporated. These data demonstrated that during the ATPase cycle, both NBDs bind ATP. During gel filtration, which takes 10–30 min, no nucleotides, but only the phosphate is released from the formed dimer. Thus

these results demonstrate that both nucleotides have to be bound to both monomers before the stable dimer is formed, and that the two nucleotides then remain associated during the entire hydrolysis cycle.

Surprisingly, incubation of the E599Q mutant with ATP in the presence of Mg^{2+} at 30 °C resulted in slow hydrolysis of ATP, indicating that the E599Q mutant still hydrolyzes ATP (but at a 3000-fold reduced rate compared with the wild-type). This enabled us to explore the nucleotide composition of the mutant E599Q dimer of Mdl1p under hydrolyzing conditions. After prolonged incubation in the presence of limiting amounts of ATP, an intermediate state, which contained one ATP and one ADP was formed. This intermediate state could be isolated for a prolonged period of time. This state was dependent on ATP limiting conditions, since in the presence of excess of ATP a state with two ATPs was isolated (data not shown). Such an asymmetric ATP/ADP state can only arise if the hydrolysis of the second ATP is slower than hydrolysis of the first, and suggests that the ATP hydrolysis occur by a sequential mechanism. Recently, mutants in the conserved glutamate in human P-gp were shown to be able to hydrolyze one ATP molecule but unable to initiate a second ATP hydrolysis (20, 21, 28). The E599Q NBD of Mdl1p, however, catalyzes multiple turnovers. This is probably caused by dimer dissociation of the intermediate state with one ATP and one ADP, and rebinding of ATP by the monomers, starting a new cycle in which again only one ATP is hydrolyzed. Indeed under ATP limiting condition this dimer dissociates before it hydrolyzed the second ATP (Fig. 6*D*, *left panel*). We tried to examine the hydrolysis of the second ATP by following the fate of the nucleotides after re-isolation of the dimer using gel filtration. Unfortunately, after dilution by gel filtration, the association-dissociation kinetics of the equilibrium between the monomeric and dimeric states and the rate of ATP hydrolysis were of the same order ($t_{1/2}$ ~30 min), severely complicating our analysis. To examine the coupling of ATP hydrolysis, P_i release, and dimer dissociation in detail, either methods with a better time resolution, or an E599Q mutant with a faster hydrolysis rate should be used.

Interestingly, an asymmetric state with equimolar amounts of ATP and ATPγS was also observed after incubation of the E599Q mutant with ATP and ATPγS into the dimer. This resulted in incorporation of one ATPγS molecule per dimer (data not shown). The wild-type protein did not incorporate ATPγS. This suggests that binding of ATPγS to the NBD disturbs the dimer-dimer interface. The E599Q mutant seems to retain its ability to form a dimer, if only one ATPγS is bound, while the wild-type protein cannot accommodate the ATPγS in the dimer. The γ-phosphate contacts residues in both NBDs, thus stabilizing the dimer. Small changes in the NBD around the γ-phosphate thus strongly influence the ability of the NBD to form dimers, and the wild-type protein seems more affected by this than the E599Q mutant.

Published crystal structures of NBDs with a dimeric architecture showed high symmetry of the two monomers and equal occupation of both nucleotide-binding sites (14, 17) even in the full-length structure of BtuCD (13). However, based on vanadate trapping experiments combined with 8-azido-ATP photolabeling, for P-gp and homologues a model was proposed in which only one NBD hydrolyzes ATP at a time, but in an alternating manner (35, 36). Under hydrolysis conditions, it was shown for P-gp as well as for $MalFGK_2$ that 8-azido-ATP photolabeling of a BeF_x- or vanadate-trapped state resulted in approximately one [α-^{32}P]ADP bound per dimer (23, 37, 38, 39). This stoichiometry of the dimer is in contrast to our data. For all NBD dimers isolated we find two nucleotides. Also in the BeF_x-trapped state we obtained two [α-^{32}P]ADPs bound per dimer. This state contradicts the alternating-site model. Our biochemical data is however supported by the observed nucleotide occupancy in the crystal structures.

In summary, we have isolated three different intermediate states of the ATP hydrolysis cycle, containing either two ATPs, one ATP and one ADP, or two ADPs. Based on our experimental data we propose the processive clamp model, which is depicted in Fig. 7. As a first step in the ATPase cycle, ATP binds to the monomeric NBD. Since the ATP concentrations in the cell (for Mdl1p, in the mitochondrial matrix) are far above the K_d value determined for ATP binding, almost all of the NBDs would be in the ATP bound state under physiological conditions. Upon ATP binding, both NBDs associate to a dimer. This state is in a dynamic equilibrium between the association, dissociation as well as hydrolysis of the ATP. As a next step, one ATP is hydrolyzed. In the experiments with the E599Q mutant, hydrolysis of the second ATP could not be observed, because in the ATP/ADP bound state, the dimer is unstable and dissociates. In the slow hydrolysis cycle of the E599Q mutant, the dissociated monomers are reloaded with ATP and in a next cycle again one ATP is hydrolyzed. Hydrolysis in the wild-type NBD is however 3000-fold faster and here two ADPs can be trapped in the dimer. Based on the much faster kinetics of ATP hydrolysis and the trapping of two ADPs in the wild-type NBD, we suggest that both ATPs be hydrolyzed sequentially in one cycle, in a processive mode. Finally, after both ATPs are hydrolyzed, the dimer disassembles and both ADPs are released. How such a hydrolysis cycle is exactly coupled to transport of the substrate and conformational changes of the TMDs, and whether the TMDs superimpose a regulatory effect on the NBDs remains unknown and requires further investigations. Smith *et al.* (14) proposed a possible model for the coupling of ATP hydrolysis to substrate transport. In this model, the TMDs of the non-substrate bound transporter forced the NBDs to remain in their monomeric state. Binding of the substrate to the high affinity site in the TMDs changes the conformation of the TMDs and removes the restrain on the NBD. Only then, the ATP-loaded NBDs form a dimer. Formation of the dimer forces a change on the TMDs and displaces the substrate-binding site, which results in transport of the substrate across the membrane. Hydrolysis of the ATP and dissociation of the dimer subsequently resets the transporter. In such a model, which fits to both the crystal structures and our experimental data, the formation of the ATP-bound dimer would be the power stroke. This would also explain how substrate binding induces ATPase activity by transmission of conformational changes between TMDs and NBDs (36, 40, 41, 42). The mechanism of the coupling of ATP hydrolysis and substrate transport requires however further investigation.

Acknowledgments—We thank Lutz Schmitt and Rupert Abele for stimulating discussions and careful reading of the manuscript, and Silke Hutschenreiter for performing the MALDI-TOF-MS analysis.

REFERENCES

1. Higgins, C. F. (1992) *Annu. Rev. Cell Biol.* **8,** 67–113
2. Lankat-Buttgereit, B., and Tampé, R. (2002) *Physiol. Rev.* **82,** 187–204
3. Young, L., Leonhard, K., Tatsuta, T., Trowsdale, J., and Langer, T. (2001) *Science* **291,** 2135–2138
4. Arnold, I., and Langer, T. (2002) *Biochim. Biophys. Acta.* **1592,** 89
5. Holland, I. B., and Blight, M. A. (1999) *J. Mol. Biol.* **293,** 381–399
6. Walker, J. E., Saraste, M., and Gay, N. J. (1982) *Nature* **298,** 867–869
7. Hung, L. W., Wang, I. X., Nikaido, K., Liu, P. Q., Ames, G. F., and Kim, S. H. (1998) *Nature* **396,** 703–707
8. Diederichs, K., Diez, J., Greller, G., Muller, C., Breed, J., Schnell, C., Vonrhein, C., Boos, W., and Welte, W. (2000) *EMBO J.* **19,** 5951–5961
9. Karpowich, N., Martsinkevich, O., Millen, L., Yuan, Y. R., Dai, P. L., MacVey, K., Thomas, P. J., and Hunt, J. F. (2001) *Structure (Camb).* **9,** 571–586
10. Yuan, Y. R., Blecker, S., Martsinkevich, O., Millen, L., Thomas, P. J., and Hunt, J. F. (2001) *J. Biol. Chem.* **276,** 32313–32321
11. Gaudet, R., and Wiley, D. C. (2001) *EMBO J.* **20,** 4964–4972
12. Chang, G., and Roth, C. B. (2001) *Science* **293,** 1793–1800
13. Locher, K. P., Lee, A. T., and Rees, D. C. (2002) *Science* **296,** 1091–1098

14. Smith, P. C., Karpowich, N., Millen, L., Moody, J. E., Rosen, J., Thomas, P. J., and Hunt, J. F. (2002) *Mol. Cell* **10,** 139–149
15. Schmitt, L., and Tampé, R. (2002) *Curr. Opin. Struct. Biol.* **12,** 754–760
16. Kerr, I. D. (2002) *Biochim. Biophys. Acta.* **1561,** 47–64
17. Hopfner, K. P., Karcher, A., Shin, D. S., Craig, L., Arthur, L. M., Carney, J. P., and Tainer, J. A. (2000) *Cell* **101,** 789–800
18. Fetsch, E. E., and Davidson, A. L. (2002) *Proc. Natl. Acad. Sci. U. S. A.* **99,** 9685–9690
19. Loo, T. W., Bartlett, M. C., and Clarke, D. M. (2002) *J. Biol. Chem.* **277,** 41303–41306
20. Hrycyna, C. A., Ramachandra, M., Germann, U. A., Cheng, P. W., Pastan, I., and Gottesman, M. M. (1999) *Biochemistry* **38,** 13887–13899
21. Sauna, Z. E., Muller, M., Peng, X. H., and Ambudkar, S. V. (2002) *Biochemistry* **41,** 13989–14000
22. Morbach, S., Tebbe, S., and Schneider, E. (1993) *J. Biol. Chem.* **268,** 18617–18621
23. Urbatsch, I. L., Sankaran, B., Weber, J., and Senior, A. E. (1995) *J. Biol. Chem.* **270,** 19383–19390
24. Nikaido, H. (2002) *Proc. Natl. Acad. Sci. U. S. A.* **99,** 9609–9610
25. Nikaido, K., Liu, P. Q., and Ames, G. F. (1997) *J. Biol. Chem.* **272,** 27745–27752
26. Booth, C. L., Pulaski, L., Gottesman, M. M., and Pastan, I. (2000) *Biochemistry* **39,** 5518–5526
27. Fisher, A. J., Smith, C. A., Thoden, J. B., Smith, R., Sutoh, K., Holden, H. M., and Rayment, I. (1995) *Biochemistry* **34,** 8960–8972
28. Urbatsch, I. L., Julien, M., Carrier, I., Rousseau, M. E., Cayrol, R., and Gros, P. (2000) *Biochemistry* **39,** 14138–14149
29. Moody, J. E., Millen, L., Binns, D., Hunt, J. F., and Thomas, P. J. (2002) *J. Biol. Chem.* **277,** 21111–21114
30. Davidson, A. L., Laghaeian, S. S., and Mannering, D. E. (1996) *J. Biol. Chem.* **271,** 4858–4863
31. Liu, P. Q., Liu, C. E., and Ames, G. F. (1999) *J. Biol. Chem.* **274,** 18310–18318
32. Nikaido, K., and Ames, G. F. (1999) *J. Biol. Chem.* **274,** 26727–26735
33. Kennedy, K. A., and Traxler, B. (1999) *J. Biol. Chem.* **274,** 6259–6264
34. Annereau, J. P., Ko, Y. H., and Pedersen, P. L. (2003) *Biochem. J.* **371,** 451–462
35. Senior, A. E., and Gadsby, D. C. (1997) *Semin. Cancer Biol.* **8,** 143–150
36. van Veen, H. W., Margolles, A., Muller, M., Higgins, C. F., and Konings, W. N. (2000) *EMBO J.* **19,** 2503–2514
37. Senior, A. E., al-Shawi, M. K., and Urbatsch, I. L. (1995) *FEBS Lett.* **377,** 285–289
38. Sankaran, B., Bhagat, S., and Senior, A. E. (1997) *Biochemistry* **36,** 6847–6853
39. Sharma, S., and Davidson, A. L. (2000) *J. Bacteriol.* **182,** 6570–6576
40. Neumann, L., Abele, R., and Tampé, R. (2002) *J. Mol. Biol.* **324,** 965–973
41. Gorbulev, S., Abele, R., and Tampé, R. (2001) *Proc. Natl. Acad. Sci. U. S. A.* **98,** 3732–3737
42. Chen, M., Abele, R., and Tampé, R. (May 30, 2003) *J. Biol. Chem.* 10.1074/jbc.M302757200